

# New methods of real-time control imaging for ion therapy

D. Dauvergne<sup>1\*</sup>, M. Battaglia<sup>1</sup>, G. Montarou<sup>2</sup>, E. Testa<sup>1</sup>

<sup>1</sup>IPNL, Université de Lyon, F-69003 Lyon; Université Lyon 1 and IN2P3/CNRS, UMR 5822, F-69622 Villeurbanne, France ; <sup>2</sup>LPC Clermont-Ferrand, IN2P3, Université Blaise Pascal, Clermont-Ferrand, France

\* e-mail address: [d.dauvergne@ipnl.in2p3.fr](mailto:d.dauvergne@ipnl.in2p3.fr)

## Abstract

We present the ongoing studies aiming at providing a real-time control of the dose distribution during ion therapy. These studies are undertaken in the frame of the National and Rhône-Alpes Regional Research Programs for Hadrontherapy. We aim at implementing combined modalities for real-time quality control of the deposited dose for future therapy centers. Several modalities are under development within this research program. Improvements on Positron Emission Tomography (PET) can be obtained by means of Time of Flight, using fast scintillators or resistive plate chambers, with dedicated readout and electronics. The in-beam prompt gamma imaging looks very promising in view of recent preliminary results, provided Time of Flight is used to discriminate gamma from neutrons and scattered particles. A collimated detection setup or a Compton camera is envisaged. Prompt emission of light charged particles like protons is also discussed.

## Introduction

The main distinctive characteristic of ion-therapy, as compared to conventional radiotherapy, is the highly non-uniform profile of dose deposition inside the irradiated body. The dose increases gradually along the ion path to reach a steep maximum at the Bragg peak. Beyond this point, the longitudinal dose drops down quite abruptly, since only a small flux of secondary particles contribute to it. The lateral dose distribution is also quite narrow. Indeed, the transverse dispersion comes mostly from multiple scattering of the charged projectiles before stopping.

Therefore, *in vivo* 3D-imaging of the dose is of utmost importance for quality control during patient treatment, and drives a diversified R&D program which includes a variety of techniques. The uncertainty on the location of the Bragg peak in the patient may be large, as much as 1 cm in some cases, due to the stoichiometric calibration of the CT images used in treatment planning, as well as to possible morphologic changes occurring between CT and treatment and during the treatment itself, such as patient mispositioning, tumour shrinkage, weight change and organ motion. Since no primary radiation emerges from the patient, *in vivo* imaging must be performed exploiting secondary radiations. To be useful, such radiation must emerge from the patient, *i.e.* to have a weak interaction probability, and be correlated to the primary beam dose distribution. This information on the electromagnetic energy deposition (the LET) can be extracted from hadronic interactions [1,2,3].

A significant effort has been already deployed to address these issues and several techniques have been proposed and tested. The present paper reviews the various developments underway on the on-line beam dose deposition imaging that are performed within the Rhône-Alpes Regional Program for Research in Hadrontherapy, with the motivation of providing new methods for quality control in future therapy centers like ETOILE in Lyon. These developments include improvement of in-beam Positron Emission Tomography (IBPET) by means of time of flight, in-beam imaging by prompt gamma-rays and secondary charged particles.

## Positron Emission Tomography

So far the only operating control system available during ion therapy is PET, which is based on the observation of the radiation from radioisotopes formed in the nuclei fragmentation process, namely the annihilation of  $\beta^+$  particles into two photons [3,4,5,6,7]. The main  $\beta^+$  radioactive isotopes formed during proton or carbon irradiation are  $^{11}\text{C}$ ,  $^{15}\text{O}$  and  $^{10}\text{C}$ , with respective half-lives of 20 min, 2 min and 20 s. The suitability of various light ion beams for PET imaging has been studied at GSI and HIMAC [8,9,10]. Although only the target nuclei undergo fragmentation during proton therapy, the absolute rate of  $\beta^+$  emission induced during a treatment is higher by a factor of 3-5 for proton than for carbon irradiation, where also projectile fragmentation occurs, due to the larger fluence of protons required to provide the same effective dose.

The relatively short radioisotope lifetimes cited above make IBPET very attractive. This is the solution that was promoted by Enghardt *et al.* [11] with the dual-head PET BASTEI (Beta Activity Measurements at the Therapy with Energetic Ions) that has been installed at the GSI pilot project and has demonstrated its ability to provide a control of neck and head irradiations with carbon ions. The IBPET was used at GSI until 2008, whereas most of PET devices used in ion-therapy centers are offline, which necessitates the transport of the patient immediately after the treatment. However, the relatively low induced activities [12] require the acquisition of PET data for about 10 minutes or more, which limits considerably the patient flow in routine clinical environment in the case of IBPET. In addition, the integration of an IBPET device into a treatment site has to be arranged as a limited angle scanner, in order to avoid interference with the patient positioning. This causes artefacts in the reconstructed  $\beta^+$  activity distributions which partly destroy the relationship between dose and activity. Moreover, over such a period of acquisition time, the metabolism causes a wash-out of the radioactive nuclei, which blurs the image of the implanted radioactive isotopes [13]. The low statistics problem could be circumvented by using radioactive  $^{11}\text{C}$  ion beams instead of stable ions which, in addition, provide additional therapeutic dose after implantation due to the projectile radioactivity [14]. Tomitani *et al.* have studied the biologic lifetime, *i.e.* the metabolic wash-out, of the implanted radio-elements in clinical conditions with rabbits. They reported that more than 50% of the  $\beta^+$  activity is lost within 4 minutes or less, depending on the tissue irradiated [15].

Improvements of IBPET involve mainly the use of TOF between the two detected gammas. Indeed, during heavy ion treatments, a considerable amount of activity is coming from outside the field of view of the IBPET camera. An accuracy below 200 ps FWHM would reduce considerably the region of interest to a size of the same order as the tumor volume, and therefore decrease the number of background events registered. An important issue of PET imaging is the computer procedure needed to reconstruct an image and extract information about the deposited dose [16,17]. A significant gain on the reconstruction time could be obtained by increasing the coincidence accuracy by means of TOF between the two detected photons. This increase in image processing speed arises from the possibility to calculate at once the point of positron annihilation as soon as the coordinates of the hit detectors and the TOF information are known. Such an algorithm needs to process one single iteration through the collected data, unlike standard iterative reconstruction algorithms. Thus this would also reduce limited solid angle artifacts and open the way to quantitative imaging.

Lanthanum halide ( $\text{LaBr}_3$ ) scintillating crystals can in principle reach such  $10^{-11}\text{s}$  time resolution. For the readout of the scintillating material, two alternatives could be explored: fast, position-sensitive photomultipliers having sub-ns rise times, or the recently developed solid state Silicon PhotoMultiplier (SiPM). The SiPMs operate in the Geiger mode due to the avalanche nature of their signal, and they have a fast response time with nominal resolution of 50 ps or better. Unlike photomultipliers, SiPMs are not sensitive to magnetic fields, which makes them candidates for use in a multimodal TOF-PET – MRI. But they have not been used in large systems to date.

## Prompt gamma imaging

Since the probability for prompt gamma emission is expected to be of the same order as that for fragmentation, gamma imaging may be regarded as a competitive technique to provide real-time information about the local dose [18,19,20] both for proton and carbon ion therapy.

Prompt gamma-rays are emitted by excited fragments with sufficiently small decay times so that the largest part of the photons are emitted in flight, keeping somewhat the information on the nuclear fragmentation location.

However, measuring prompt gamma during a therapy treatment is not straightforward, since a major source of background arises from the emission of other secondary species like neutrons and light fragments, and also from Compton scattering of photons emitted in all directions. In particular, neutrons have a high multiplicity and high scattering probability in surrounding materials, and they may not be correlated to the ion path. Therefore, various alternatives are offered to provide selective information about the prompt gamma emission profile.

### 1. Collimated gamma-camera

The first one consists in a selective collimation and shielding. This method was followed by Min *et al* [18] during proton irradiation of a water phantom target. Using a scanning system based on a thick lead and paraffin collimator, the authors could demonstrate that the gamma emission profile keeps correlated with the proton range in water up to projectile incident energy of 200 MeV. However, the limited solid angle imposed by the heavy and oversized collimation setup may prevent this method from being operated in a clinical environment.

### 2. Time Of Flight-gamma camera with beam tagging

In order to improve the detection efficiency and the background rejection, our group proposed a prompt gamma detection method [19,21] which uses time of flight information to discriminate between photons and massive particles. Indeed, massive particles and scattered radiations in the surrounding materials are delayed before reaching the photon detector, as compared to direct photons. The concept was tested on a carbon ion beam at GANIL, taking advantage of the pulsed structure of the incident beam, 1 ns pulse each 80 ns. Figure 1 shows a 2D-spectrum of the energy detected by a collimated scintillator as a function of TOF for a  $^{13}\text{C}$  ion

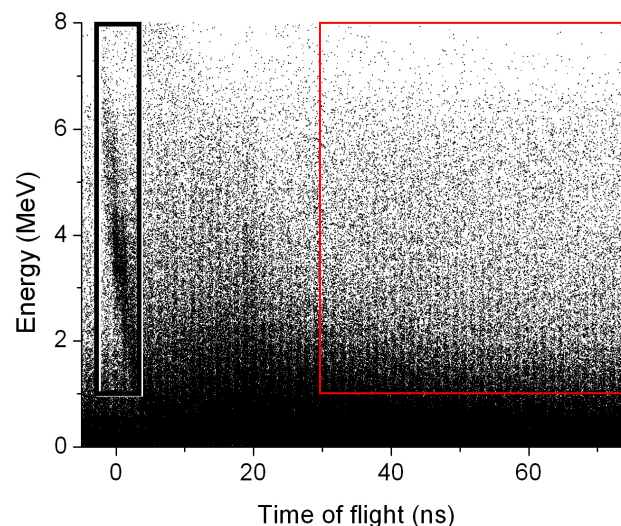


Figure 1. Two-dimensional spectrum of the  $\gamma$ -equivalent energy deposited in the NaI(Tl) detector as a function of the time of flight. The collimated scintillator aims at a location at the middle of the ion path (detection angle  $\theta=90^\circ$ ) for a 74 MeV/u carbon ion beam inside a PMMA target. The left rectangle corresponds to a selection of prompt  $\gamma$ -rays, and the right one to a neutron selection [21].

beam energy of 74 MeV/u impinging a thick PMMA target. The detector was located at  $90^\circ$  from the beam axis, at a distance of 60 cm from the target, with a narrow collimation slit (2 mm). The detected prompt gamma photons appear as a vertical band at short TOF values (the small drift with energy is due to electronics artifacts). However they account for only a minor fraction of the detected particles, which are dominated by neutrons.

The feasibility of the method is shown in Figure 2 which gives the longitudinal profile of the measured rates corresponding to the selections of prompt gammas only and of neutrons, above a given energy threshold, corresponding to the selection cuts highlighted in Figure 1. A photography of the irradiated sample shows clearly the beam range by means of the visible damage in the target. The Bragg peak corresponds to the sharp defect accumulation at the end of the range. The photon profile is well correlated to the ion range, whereas that for neutrons steadily increases with depth. Further studies performed at higher beam energies at GSI confirm that the correlation between prompt gamma yields and dose profile is preserved for carbon ions with longer ranges (in this case, the TOF was triggered by a thin scintillator intercepting the low intensity beam). This makes the proposed method feasible for the typical energies of carbon ion therapy.

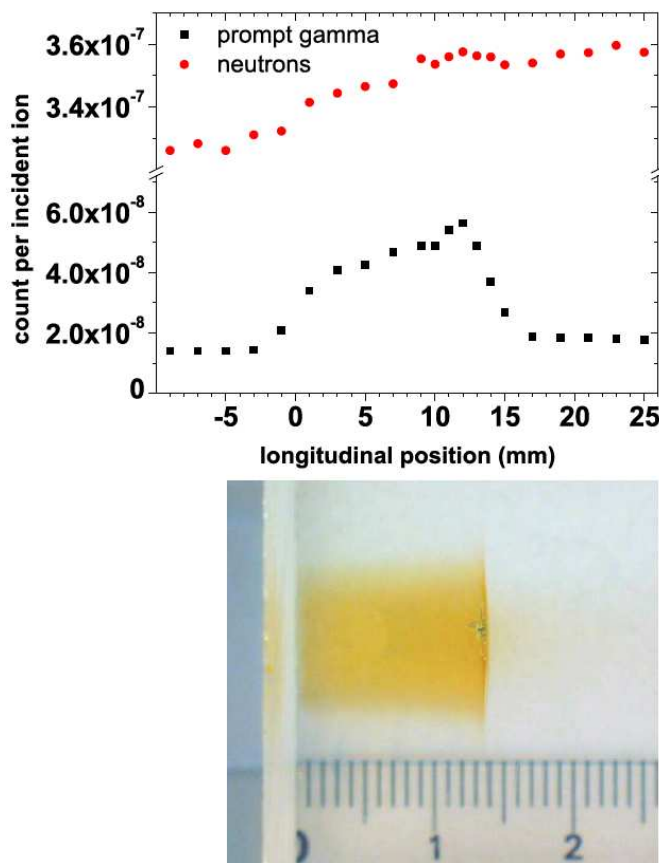


Figure 2: Detection rates as a function of the longitudinal position  $z$  obtained for the two different selections on the time of flight TOF and the energy deposited  $E$  in the detector indicated in Figure 1: photon selection (squares) and neutron selection (circles) [19]. Bottom: picture of the irradiated PMMA target.

The absolute photon yields measured are encouraging in view of designing a real-time control device during therapy. Although the solid angle of the collimated detector was small in these experiments, one can extrapolate the observed yields in view of a more efficient detection device. By increasing the solid angle by two orders of magnitude or more – which is made possible by minimizing the passive shielding against neutrons – enough contrast between the irradiated and non-irradiated zones should be observed within a few

seconds exposure, thus allowing a real-time control during patient treatments. These feasibility studies are combined with GEANT 4 simulations which, in a first step, provide direct comparison with theoretical models, and, in a second step, will help for designing an optimized detection setup.

A 2D-transverse position information on the incoming ions is required to complete the longitudinal profile. The incident beam tagging, in both time and transverse position, requires the development of a fast position-sensitive detector, with a count rate capability of  $10^8$  ions/s and 1 ns time resolution. A prototype, consisting in a scintillating fibers hodoscope read out by flat-panel PMs, is under development at IPN Lyon. Since scintillating fibers are affected by radiation damage on the intense primary beam, an alternative technology under consideration consists in polycrystalline diamond detectors, produced by Chemical Vapor Deposition (CVD) [22,23,24]. Such detectors exhibit quite good radiation tolerance. Diamond detectors can be obtained with large area, 1 ns or less timing resolution, and with x and y segmentation in order to cope with the high count rate and provide position information in an event by event mode.

Although 3D-data are recorded by this method, the limited statistics imposed by the collimation may restrict the quantitative imaging to 1D or 2D projections. Nevertheless, this represents a considerable breakthrough in the quality control for ion-therapy, since this information is not yet available.

### 3. Compton camera

A considerable improvement in the detection of prompt photons can be achieved with a Compton Camera. The system can be considered to function like a standard  $\gamma$ -camera where the performance-limiting absorbing collimator is replaced by an electronically-operating collimator. A gamma ray emitted undergoes a Compton scattering in a first (scatter) detector, and the scattered photon which interacts in a secondary (absorption) detector conveys information on the direction of the incoming gamma ray. Information on energy deposition and interaction position in these detectors confines the possible incoming path of the initial gamma ray to lie on a cone, whose apex is the interaction position in the scatter detector. Compton cameras are currently under development worldwide, for application in gamma astronomy, medical imaging or homeland security [25,26]. For the case of prompt gamma imaging, where the source is extended and the energy spectrum is broad, the position and energy resolutions of the scatter detector are the key issues. A stack of Si(Li) detectors is envisaged [27]. In parallel, a specific reconstruction strategy, based on a precise iterative and fast analytic reconstruction algorithm, is under development.

The Compton camera solution, with an efficiency increase of nearly two orders of magnitude compared to a collimated gamma-camera, is a much more ambitious and promising technology allowing online real 3D-imaging of the dose. Beyond the R&D challenges, a successful development of such a device would represent a major breakthrough in ion therapy imaging [28].

### Charged Particle Imaging

The analysis of charged particles, created in the ion interaction and fragmentation processes, which emerge from the patient offer a potential complementary opportunity to determine the points of interaction of the primary beam. The principle, which resembles that of vertex identification in fixed target particle physics experiments, is to reconstruct the trajectories of the particles emerging from the interactions by a precise charged particle hodoscope and extrapolate them back to their production point. The intercept of the trajectory of individual particle with the line of flight of the incoming ion, has been proposed in the context of the CNAO-sponsored AQUA quality assurance program and should provide a determination of the point of interaction with a resolution of a few mm, limited by multiple scattering and the effect of secondary interactions. Further, the possibility to use multiple particle tracks produced at the same interaction points would open the way to a real vertex reconstruction, intrinsically able to give a three-dimensional measurement

of the point of interaction with accuracies of the order of 1 mm. A program of simulation validation using data for the secondary proton yield and energy spectra and of secondary proton tracking and vertexing is currently being carried out jointly by IPN Lyon and TERA. In a second phase, a demonstration of the 3D reconstruction capabilities of these methods on a carbon ion beam using a small scale charged particle tracker and calorimeter is envisaged.

## Conclusion

A diversified research program on online dose monitoring during ion therapy is currently ongoing, supported by the Rhône Alpes Regional Program for Research in Hadrontherapy. The program is carried out in the perspective of providing advanced and combined solutions for the treatment quality insurance to the ETOILE ion therapy, which is expected to treat the first patients by late 2012. These studies are also supported by CNRS-GDR MI2B. They are part of the European project ENVISION proposed by the ENLIGHT++ research network in the frame of the FP7.

## References

- [1] Schardt D, Schall I, Geissel H *et al.* Nuclear fragmentation of high-energy heavy-ion beams in water. *Adv. Space Res.* 1996;17: 87-94.
- [2] Inaniwa T, Kohno T, Tomitani T *et al.* Experimental determination of particle range and dose distribution in thick targets through fragmentation reactions of stable heavy ions. *Phys. Med. Biol.* 2006; 51:4129-4146.
- [3] Matsufuji N, Fukumura A, Komori M *et al.* Influence of fragment reaction of relativistic heavy charged particles on heavy-ion radiotherapy, *Phys. Med. Biol.* 2003; 48: 3393-3403.
- [4] Enghardt W, Crespo P, Fiedler F *et al.*, Charged hadron tumour therapy monitoring by means of PET *Nucl. Instrum. Methods Phys. Res. A*, 2004, 525, 284-288.
- [5] Parodi K, Bortfeld T, Enghardt W *et al.* PET imaging for treatment verification of ion therapy: Implementation and experience at GSI Darmstadt and MGH Boston. *Nucl. Instrum. and Meth. A.* 2008; 591: 282-286.
- [6] Solevi P, Study of an in-beam PET system for CNAO, the National Centre for Oncological Hadrontherapy. 2007; PhD thesis, University of Milano.
- [7] Nishio T, Miyatake A, Inoue K *et al.*, Experimental verification of proton beam monitoring in a human body by use of activity image of positron-emitting nuclei generated by nuclear fragmentation reaction. *Radiol Phys Technol.* 2008; 1:44-54
- [8] Iseki Y, Mizuno H, Futami Y, Positron camera for range verification of heavy-ion radiotherapy, *Nucl. Instrum. Methods. Phys. Res. A* 2003;515: 840-849
- [9] Pawelke J, Enghardt W, Haberer T *et al.* In-beam PET imaging for the control of heavy-ion tumour therapy. *IEEE Trans. Nucl. Sci.* 1997;44:1492-1498.
- [10] Inaniwa T, Tomitani T, Kohno T and Kanai T, Quantitative comparison of suitability of various beams for range monitoring with induced  $\beta^+$  activity in hadron therapy. *Phys. Med. Biol.* 2005; 50: 1131-1145.
- [11] Enghardt W, Debus J, Haberer T *et al.* The application of PET to quality assurance of heavy-ion tumor therapy. *Strahlenther Onkol.* 1999; 175-S2: 33-36.
- [12] Enghardt W, Parodi K, Crespo P *et al.*, Dose Quantification from In-Beam Positron Emission Tomography, *Rad. Oncol.* 2004; 73:S96-98

- [13] Fiedler F, Priegnitz M, Jülich R *et al.*, In-beam PET measurements of biological half-lives of  $^{12}\text{C}$  irradiation induced  $\beta^+$ -activity. *Acta Oncol.* 2008; 47:1077-1086.
- [14] Kitagawa A, Furusawa Y, Kanai T *et al.*, Medical application of radioactive nuclear beams at HIMAC. *Rev. Sci. Instrum.* 2006; 77: 03C105.
- [15] Tomitani T, Pawelke J, Kanazawa M *et al.*, Washout studies of  $^{11}\text{C}$  in rabbit thigh muscle implanted by secondary beams of HIMAC. *Phys. Med. Biol.* 2003; 48:875-889.
- [16] Inaniwa T, Kohno T, Yamagata F *et al.*, Maximum likelihood estimation of proton irradiated field and deposited dose distribution. *Med. Phys.* 2007; 34:1684-1692.
- [17] Shakirin G, Crespo P, Enghardt W, A Method for System Matrix Construction and Processing for Reconstruction of In-Beam PET Data. *IEEE Trans. Nucl. Sci.* 2007;54:1710.
- [18] Min C H, Kim C H, Youn M Y, Kim J W, Prompt gamma measurements for locating the dose falloff region in the proton therapy. *Appl. Phys. Lett.* 2006;89:183517.
- [19] Testa E, Bajard M, Chevallier M *et al.*, Monitoring the Bragg peak location of 73 MeV/u carbon ions by means of prompt gamma-ray measurements. *Applied Physics Letters*, 2008, 93, 093506
- [20] Polf J C, Peterson S, Ciangaru G *et al.*, Prompt gamma-ray emission from biological tissues during proton irradiation: a preliminary study. *Phys. Med. Biol.* 2009; 54 :731–743
- [21] Testa E, Bajard M, Chevallier M *et al.*, Dose profile monitoring with carbon ions by means of prompt-gamma measurements. To be published in *Nuclear Instruments and Methods B*. Preprint available online at <http://hal.archives-ouvertes.fr/hal-00283936/fr/>
- [22] Descamps C, Tromson D, Tranchant N *et al.*, Clinical studies of optimised single crystal and polycrystalline diamonds for radiotherapy dosimetry. *Radiation Measurements* 2008; 43: 933-938.
- [23] Bergonzo P, Brambilla A, Tromson D *et al.*, Diamond as a tool for synchrotron radiation monitoring: beam position, profile, and temporal distribution. *Diamond and Related Materials* 2000; 9: 960.
- [24] Rebisz M, Alternative methods for heavy-ion therapy dosimetry. Thesis, Heidelberg, 2007.
- [25] Tanimori T, Hattori K, Kabuki S *et al.*, Advanced Compton Camera with the ability in electron tracking based on Micro Pixel Gas Detector for Medical Imaging Nuclear Science Symposium Conference Record, 2006. *IEEE* 2006; 6:3870–3874.
- [26] Protic D, Hull EL, Krings T, Vetter K. Large volume Si(Li) orthogonal strip detectors for Compton effect - based instruments. *IEEE Trans. Nucl. Sci.* 2005; 52:3181-3185.
- [27] Walenta AH, Brill AB, Castoldi A *et al.*, Vertex determination in a stack of Si-drift Detectors for High Resolution Gamma-ray Imaging. *IEEE Trans. Nucl. Sci.* 2005; 52:1434-1438
- [28] Feng Y, Baciak J, Haghghat A, A Design of Compton Cameras for Imaging Gamma Emission in Proton Therapy, 50th AAPM Annual Meeting, July 27-31, 2008, Houston, Texas, 2008. Available online: <http://www.aapm.org/meetings/amos2/pdf/35-9435-45230-12.pdf> (29.09.2008)